THE JOURNAL OF COMPARATIVE NEUROLOGY 447:114–127 (2002)

Retinofugal Projections in the Short-Tailed Opossum (*Monodelphis domestica*)

DIANNA M. KAHN AND LEAH KRUBITZER*
Center for Neuroscience and Department of Psychology, University of California, Davis, Davis, California 95616

ABSTRACT

In the current investigation, retinofugal projections to midbrain and thalamic nuclei of *Monodelphis domestica* were investigated using wheat-germ agglutinin conjugated to horseradish peroxidase (WGA-HRP). Large intraocular injections of WGA-HRP were placed into the eye, and patterns of labeled axon terminals were related to nuclear boundaries in tissue that was stained for Nissl or reacted for cytochrome oxidase (CO). Our results demonstrate that the major projection from the retina is to the contralateral dorsal lateral geniculate nucleus (LGNd) and the superior colliculus (SC). Connections were also observed with the contralateral pretectal nucleus (PRT), the lateral posterior nucleus (LP), and the ventral division of the lateral geniculate nucleus (LGNv). Ipsilateral connections were with the LGNv and LGNd. These findings are consistent with reports in other marsupials as well as with studies in a number of eutherian mammals. Thus, there appears to be a common pattern of retinofugal projections that all mammals share, probably due to retention from a common ancestor. However, some features such as a lack of ipsilateral input to the SC (which are absent only in certain species like *Monodelphis*, platypus, and echidnas) may represent a primitive state retained from a common ancestor. When comparisons of retinofugal connections and LGNd organization are made across taxa, three types of organization are observed: a homogenous LGNd with a high degree of binocular overlap of projections; a partially differentiated LGNd with some segregation of eye-specific inputs; and a fully segregated structure with a large degree of segregation of eye-specific inputs. We discuss the factors that contribute to the organization observed in extant mammals and conclude that phylogeny and lifestyle appear to be the underlying factors contributing to the organization of the LGNd. J. Comp. Neurol. 447:114–127, 2002.

Indexing terms: lateral geniculate nucleus; evolution; marsupials; visual system; superior colliculus; WGA-HRP

One of the challenges when examining any particular neural structure is to determine the sources that contribute to its present organization and whether some subset of its morphological features is requisite for its function. Is a specific type of organization necessary to perform a particular task, or are some features of organization epiphenomenal and the result of underlying, highly constrained, developmental regimes? For example, are ocular dominance columns in the primary visual area of primates necessary for binocular vision? Are the barrels in the primary somatosensory cortex of some rodents necessary for a specialized type of tactile discrimination? In the case of the dorsal lateral geniculate nucleus (LGNd), is the striking laminar organization observed in a number of species requisite for some fundamental function?

When examining the LGNd, one is struck by the differences in morphology that different species possess, as well as the differences in the segregation of inputs from the two eyes (Kaas et al., 1978; Sanderson et al., 1984, 1987). However, within the realm of possible organizations, the

Grant sponsor: NINDS; Grant number: 1 T01 NS35103-04A1.

*Correspondence to: Leah Krubitzer, Center for Neuroscience, 1544 Newton Ct., Davis, CA 95616. E-mail: lakrubitzer@ucdavis.edu

Received 30 July 2001; Revised 8 November 2001; Accepted 17 January 2002

DOI 10.1002/cne.10206

Published online the week of April 15, 2002 in Wiley InterScience (www.interscience.wiley.com).

TABLE 1. Relative Amounts of Labeled Axon Terminals in Retinal Targets in Normal Animals

Case no.	Transport time (days)	Labeled targets										
		LGNd	LGNv	SC	LP	PRT	NOT	NT	MTN	Ipsi LGNd	Ipsi LGNv	Ipsi NT
98-2	2	XXXX	XXX	XXXX	XX	XX	XXX		XXX	XXX	XX	
98-14	2	XXX		XX		X		XX				XX
99-44	7	XXX	XX	XXX	X	XX	X	XX		XX	X	XX
98-27	7	XXX	X	XX	X	X	XX					
98-16	14	X	X	X	X	X						
98-23	14	XX	X	XX	X	X	XX					

X, sparse projection; XX, moderate projection; XXX, dense projection; XXXX, very dense projection.

LGNd encompasses only a few types. For instance, although some animals have highly segregated inputs from each eye and others have a large amount of binocular overlap, the way in which inputs are segregated is restricted to sets of interleaving laminae. Such observations argue that only a few sources or factors have a significant impact on the organization of the LGNd in mammals. One of the factors thought to contribute to the variation in visual system organization is the ecological niche of the animal, or the degree to which an organism depends on its visual system for survival behaviors such as prey capture and resource acquisition (Sanderson et al., 1984; Barton and Purvis, 1995; Chiel and Beer, 1997). Another factor, at least for eutherian mammals, is whether an animal is diurnal or nocturnal. This is less of an issue for prototherians, because they are exclusively nocturnal, and metatherians, which are almost exclusively nocturnal and/or crepuscular.

In eutherian mammals, cytoarchitectural lamination of the LGNd and segregation of retinal afferents into eye-specific layers is generally associated with animals with more frontally placed eyes, such as carnivores and primates. Both groups are highly dependent on visual processing for survival and their visual systems are organized in a complex fashion. For example, the LGNd of carnivores and primates consists of precisely organized eye-specific laminae, each receiving information from functionally distinct retinal cell types (Stone and Hansen, 1966; Kaas et al., 1978; see Kaas and Huerta, 1988, for review). In contrast, many animals with laterally placed eyes who often rely less on vision for resource acquisition, such as monotremes, insectivores, and rats, have a more simply organized LGNd, with little segregation of retinal inputs (Campbell et al., 1967; Campbell and Hayhow, 1971, 1972; Cunningham and Lund, 1971; Dinopoulos et al., 1987). Thus, the niche selects for the placement of the eyes, which in turn is tied to the relative activity patterns between the two eyes during development. Therefore, ecological factors and selection for placement of the eyes on the head act in concert with developmental mechanisms to generate the types of visual system organization that we observe across different mammals.

Another related factor that contributes to the organization and patterns of connections of a particular structure across species is the evolutionary history or phylogeny of the structure in question (Brauer et al., 1978; Pettigrew et al., 1989; Nieuwenhuys, 1994). During development, the presence of homologous genes and the similarities in their patterns of spatial and temporal expression presumably result in similar phenotypes. Conversely, changes in these patterns, or mutations, can cause large phenotypic differences. However, because genetic change in the form of deletions that produce viable offspring are rare, the types of observed change are rather limited. Thus, the course of future evolution in any species is restricted by the cascade of developmental events that generate the nervous system of a particular group, and presumably more closely related species would share more ontogenetic features than distantly related ones. One way to tease out the various contributions to the existing phenotype, in particular to the organization of the visual system, is to examine a number of species from a given lineage that occupy a variety of niches.

In the present investigation we examined the retinofugal connections of the South American short-tailed opossum, *Monodelphis domestica*, by injecting anatomical tracers into the eyes and examining the patterns of labeling in thalamic and midbrain structures. We compared our results with those of other marsupials and mammals in an effort to determine common features of visual system organization across groups, and the factors that may contribute to phenotypic variability in the organization of the lateral geniculate nucleus.

Abbreviations

CeM	central medial nucleus
CG	central gray
CP	cerebral peduncle
IC	inferior colliculus
IGL	intergeniculate leaflet
IML	internal medullary lamina
LGN	lateral geniculate nucleus
LGNd	lateral geniculate nucleus, dorsal division
LGNv	lateral geniculate nucleus, ventral division
LP	lateral posterior nucleus
MD	medial dorsal nucleus
MGN	medial geniculate nucleus
MTN	medial terminal nucleus
NOT	nucleus of the optic tract
NT	trochlear nucleus
ON	optic nerve
OT	optic tract
PAG	periaqueductal gray
PRT	pretectal complex
RGC	retinal ganglion cell
SC	superior colliculus
VM	ventromedial nucleus
VP	ventroposterior nucleus

MATERIALS AND METHODS

Intraocular injections

Six short-tailed opossums (*M. domestica*) were used to examine retinal projections (Table 1). Each animal was anesthetized with a cocktail of ketamine (40 mg/kg) and

xylazine (5 mg/kg) administered intramuscularly. Lidocaine was applied topically onto the eye and subcutaneously into the tissue surrounding the eye. Body temperature was maintained by placing the animal on a heating pad during the surgery and was monitored throughout the experiment. Once a surgical level of anesthesia was reached, a monocular intravitreal injection of a 4% solution of wheat-germ agglutinin conjugated to horseradish peroxidase (WGA-HRP; Sigma, St. Louis, MO) in 0.9% sterile saline was made in one eye. Injections were made by inserting the needle into the eye so that the tip of the needle could be visualized at the edge of the vitreous humor. In two cases (98-2, and 98-27) 5 μl of WGA-HRP was injected using a 10-μl Hamilton syringe with a 25-gauge needle. In four cases (98-14, 98-16, 98-23, and 99-44), a catheter needle was inserted into the opposite pole of the eye to relieve intraocular pressure while a large volume of tracer (50 μl) was injected. Immediately following the injections, an antibacterial ointment was topically applied to the eye and the animal was allowed to recover.

To study transport of WGA-HRP in this species, the first goal was to produce consistent labeling in the LGN. Initial experiments, using injections that had proved successful in other small animals, produced variable labeling of terminals in this species. To clarify these results, different transport times were adjusted to maximize intensity and density of labeling in the thalamus. We used transport times of 2, 7, or 14 days (Table 1). We found that a transport time of 2 days produced optimal staining of labeled axons in the LGN and that at 7 and 14, days the density and intensity of labeled terminals decreased.

At either 2, 7, or 14 days after injection, animals were euthanized with an intraperitoneal injection of sodium pentobarbital (250 mg/kg) and perfused transcardially with 0.9% saline and 0.1% heparin, followed by a fixative of 3% paraformaldehyde and then 3% paraformaldehyde with 10% sucrose. Following fixation, the brain was removed from the skull, and the thalamus and brainstem were dissected free from the rest of the brain and immersed in 30% sucrose overnight. The fixed, cryoprotected brains were sectioned on a freezing sliding microtome in the coronal plane at 40 μm thickness. Sections were collected in 0.1 M phosphate buffer (PB; pH 7.4). All experimental protocols were approved by the Animal Use and Care Administrative Advisory Committee of the University of California, Davis, and conformed to NIH guidelines.

Tissue processing

To visualize the WGA-HRP labeling, free-floating sections were processed with tetramethylbenzidine (TMB) using the method of Mesulam et al. (1980), as modified by Gibson et al. (1984). Alternate sections were processed for cytochrome oxidase (CO; Caroll and Wong-Riley, 1984), myelin (Gallyas, 1979) and Nissl substance.

Additionally, the extent of the injection was examined in flat-mounted retinas processed for TMB. Retinas of the uninjected eyes were also processed for TMB, as a negative control. The low levels of background staining in the control eyes were clearly distinguishable from the labeling in the injected retinas. Following perfusion, the eyes were removed from the skull, and the lens and vitreous were dissected from the retinas. The sclera and pigment epithelium were dissected away, and the retinas were reacted for TMB and then flattened using four radial cuts. Following the TMB reaction, all tissue was mounted onto gelatin-coated slides, TMB sections were dehydrated in methyl salicylate, and other sections were dehydrated in alcohol, then all slides were cleared in xylene and coverslipped using DPX (Sigma-Aldrich) mounting media.

Data analysis

TMB-reacted tissue was analyzed using polarized lenses attached to a stereomicroscope. With the aid of a camera lucida drawing tube, outlines of individual sections were drawn, along with labeled cell bodies and axon terminals. For the thalamus, each drawing included blood vessels and tissue artifacts to aid with reconstruction of the tissue. Adjacent myelin-, Nissl-, and CO-stained sections were drawn and included the outline of each section, blood vessels, tissue artifacts, and architectonic boundaries. All drawn sections were then aligned using the landmarks indicated above and were compiled into one comprehensive reconstruction. In this way, the location of WGA-HRP-labeled retinal axon terminals could be directly related to individual thalamic nuclei.

Production details

Digital photomicrographs of tissue sections were taken using a Spot RT camera and software (Diagnostic Instruments, Sterling Heights, MI). Adobe PhotoShop 6.0 software was used to make linear adjustments of brightness and contrast so that the electronic version most closely matched the tissue sections.

RESULTS

Architectonic subdivisions of the dorsal thalamus and midbrain structures

In coronally cut Nissl sections, the dorsal and ventral divisions of the lateral geniculate nucleus (LGNd and LGNv, respectively) were easily identified (Fig. 1). The darkly stained LGNd was not overtly striated; however, it appeared to have at least two major subdivisions (Fig. 1b), which have been referred to as α and β subregions in most marsupials studied (Sanderson et al., 1979; Haight and Neylon, 1981; Haight and Sanderson, 1988, 1990). Along the lateral border of the LGNd, adjacent to the optic tract, there was a region extending from the dorsal to ventral poles, comprised mainly of large cells that were moderately to darkly stained. This subregion corresponded to the LGNα region described in other marsupials. More medially, cells were smaller, lightly stained, more loosely packed, and architecturally similar to the LGNβ region described in some marsupials. We have denoted the boundary between the subregions of the LGNd with a dashed line. Unlike the situation in other marsupials (Sanderson et al., 1987), the LGNα did not appear to be further subdivided. In CO-reacted tissue, the entire LGNd was darkly stained across the nucleus (Fig. 1c).

The divisions we describe below are like those described by Jones (1985) for a variety of mammals. The wedge-shaped LGNv could be clearly distinguished immediately ventral and slightly caudal to LGNd. In Nissl-stained tissue, the LGNv was identified as a nucleus that contained small, tightly packed, darkly stained neurons (Fig. 1b). In tissue reacted for CO, the LGNv was darkly stained (Fig. 1c).

Dorsal to the LGNv and ventral to the LGNd was a small region that was cell-sparse in Nissl-stained tissue.

In CO-reacted tissue, this area was lightly stained. This region corresponds to the intergeniculate leaflet (IGL; see arrows in Fig. 1), described in some marsupials and placental mammals. In the rat, the IGL has been characterized as a subnucleus of the LGNv (Brauer et al., 1984).

The lateral posterior nucleus (LP) is an elongated nucleus whose lateral border extends approximately to the midlevel of the LGNd. In Nissl-stained sections, cells in the mid-LP were more darkly stained and slightly more densely packed than in anterior regions. The LP has been subdivided into lateral (LPL), intermediate (LPI), and medial (LPM) subnuclei in the opossum (Benevento and Ebner, 1970). However, in the present study no distinction has been made between the subdivisions of the LP.

Layers of the superior colliculus (SC) were easily identified in Nissl- stained sections (Fig. 2), in CO-reacted tissue, and in myelin-stained sections (not shown). In all staining preparations, a distinguishing feature of the SC was the appearance of alternating mediolateral stripes of light and dark layers. The most superficial layer (I), was a cell-sparse thin stripe, identified in Nissl sections by a lack of staining. Layer I reacted very darkly for CO and also appeared very dark in myelin-stained tissue. Immediately underlying layer I was the wide, cell-dense layer II. In Nissl-stained sections, cells were darkly labeled throughout the entire layer II and were relatively larger in the medial region than in the more lateral region. Layer III was narrow, and in Nissl-stained sections, cells were small and darkly labeled. The intermediate layer IV appeared similar, but cells were darker in Nissl-stained sections. The deeper layers V, VI, and VII appeared lighter, and cells were lightly stained and less densely packed. Layer III reacted very lightly for CO, as did the deeper V layer. The intermediate layer IV reacted darkly for CO.

Retinal projections

Examination of the retinal projections revealed the highest density of retinal ganglion cell axon terminals in the contralateral dorsal lateral geniculate nucleus (LGNd) and contralateral superior colliculus (SC) in all cases (Figs. 1–6). Labeled axon terminals were observed in the LGNd ipsilateral to the injected eye in 2 cases (Figs. 3, 4). In contrast, no labeled terminals were observed in the ipsilateral SC in any case. In five cases labeled terminals were observed in the contralateral pretectum (PRT), and in four of these cases, also in the nucleus of the optic tract (NOT; Figs. 3, 4; Table 1). In one case (98-2), labeled terminals were observed in the contralateral medial terminal nucleus (MTN; not shown). Surprisingly, in two cases (98-14, not shown, and 98-44; see Fig. 6), retrogradely labeled cell bodies were found in the trochlear nucleus (NT), an oculomotor nucleus. The labeled cells observed in the NT are most likely a result of retrograde

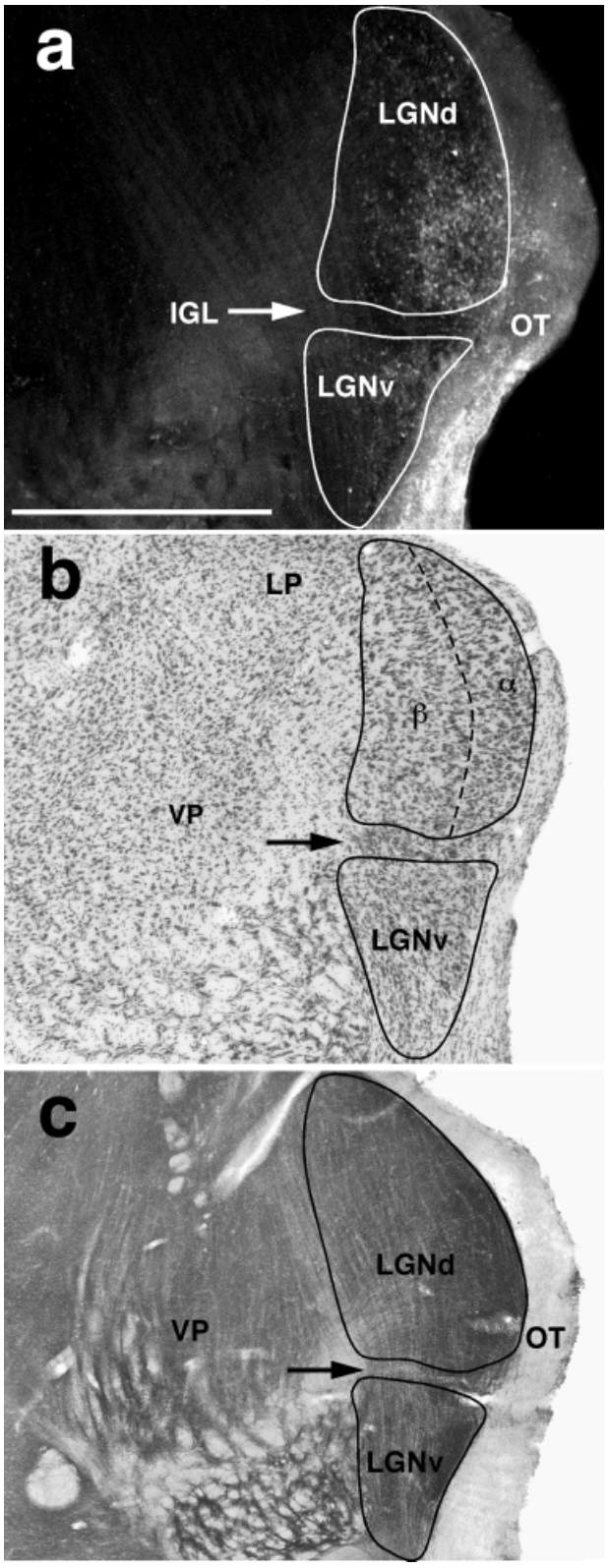

Fig. 1. Digital images of adjacent TMB-reacted (a) Nissl (b), and CO-reacted (c) coronally cut sections through the midlevels of the LGNd and LGNv in case 98-2. **a:** Solid lines denote borders of the LGNd and LGNv. WGA-HRP-labeled retinal axons and terminals were observed throughout the entire LGNd and in portions of the LGNv. **b:** Nissl staining revealed two major divisions of the LGNd (α and β). Larger, more densely packed cells characterized the α region along the optic tract of the LGNd, whereas the β region, located more medially, was more lightly stained and contained more loosely packed cells. The boundary between the two regions is marked by a dashed line. **c:** In CO-reacted tissue, the LGNd and LGNv were darkly stained. The IGL is indicated by arrows. For abbreviations, see list. Dorsal is up. Scale bar = 1 mm.

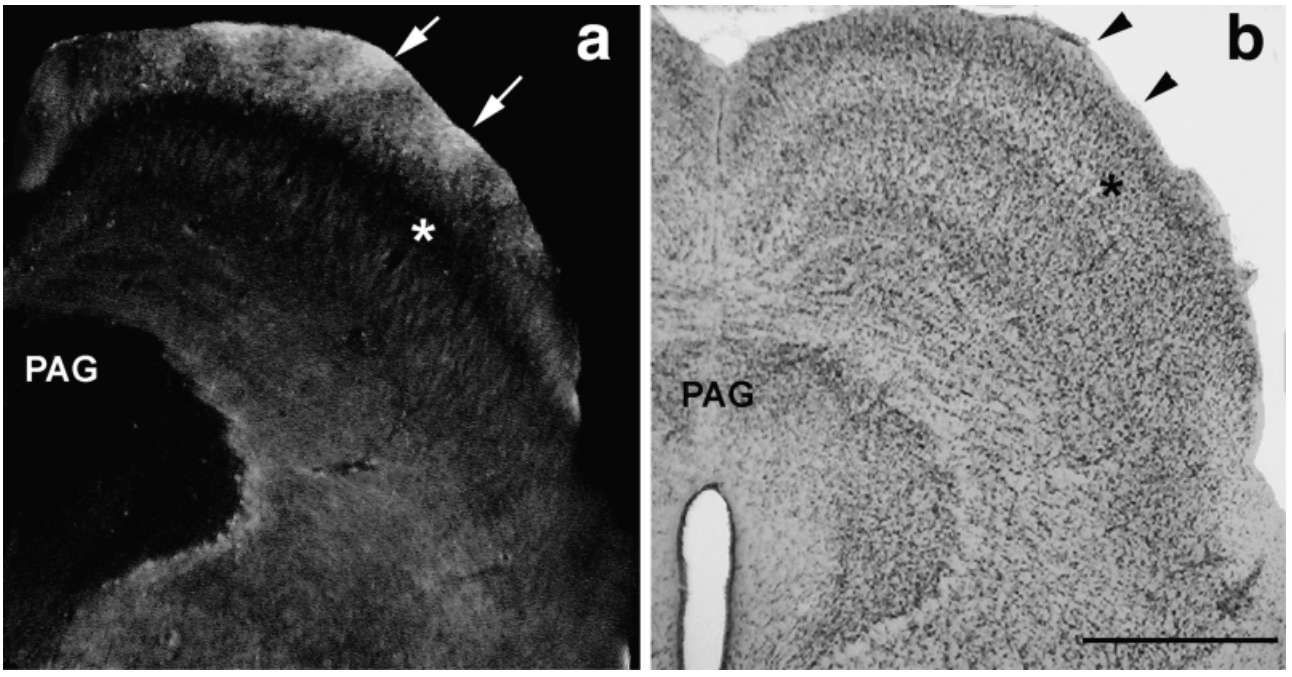

Fig. 2. Digital images of WGA-HRP labeling in the SC (**a**), along with adjacent Nissl-stained (**b**) coronally cut sections in case 98-2. Sections were taken near the midlevel of the SC. Dense patches of labeled retinal axon terminals can be seen in the superficial layers of the SC (arrows in a). Asterisks indicate a blood vessel used as a landmark to match sections within a series. Arrowheads in b indicate area of dense patches of labeling. For abbreviations, see list. Dorsal is up. Scale bar = 1 mm in b.

transport due to leakage of the tracer onto the axon terminals innervating the intraocular muscles.

Although overall labeling patterns were similar in all cases, a 2–7-day transport time appeared to be optimal in terms of density of labeled terminals. In one 2-day case (98-2) and one 7-day case (99-44), labeled terminals were observed in the ipsilateral and contralateral LGNd and LGNv (Figs. 3, 4). In the other 2-day (98-14) and 7-day (98-27, not shown) cases, labeled terminals were observed in the contralateral LGNd and LGNv only (Table 1). In all 14-day cases, labeling was considerably more sparse and was observed solely in the contralateral LGN.

Examination of the TMB-reacted retinas revealed that in four cases the WGA-HRP extended over most of the entire retina (98-2, 99-44, 98-16, and 98-14). In two retinas, spread of the dye covered approximately two-thirds of the retinal surface (98-23 and 98-27; however, see Discussion).

Lateral geniculate nucleus

In the six cases in which labeled terminals were observed, terminals were consistently located in the contralateral LGNd and LGNv (Figs. 3, 4; Table 1). Labeled terminals were dense across the mediolateral and rostrocaudal extent of the nucleus, and portions of labeled axons were dense throughout the optic tract in most cases. The labeled terminals were not strictly organized into sublaminae, although their distribution within the nucleus was not homogeneous, rather, dense patches of labeled terminals were adjacent to sparsely labeled or unlabeled patches of the nucleus. In all cases, at caudal levels of the LGNd, patches of labeled axon terminals tended to be concentrated in the ventrolateral region (Figs. 3e, 4e). In two cases (98-2 and 99-44), labeled terminals were observed in the LGNd ipsilateral to the eye injection, and this labeling was patchy and considerably less dense and tended to avoid more lateral portions of the nucleus along the optic tract.

The contralateral LGNv was labeled in five of six cases, although the density of labeled axon terminals in these cases was less dense than in the LGNd (Figs. 1, 3, 4). In these cases, labeled terminals were largely confined to the dorsolateral region of the nucleus. Dense labeling was also observed in the intergeniculate leaflet (IGL).

In two cases (98-2 and 99-44), a few labeled retinal axon terminals were observed in the ipsilateral LGNv. Label in the ipsilateral LGNv was more sparse than in the contralateral hemisphere (Figs. 3, 4). In these cases, labeled axons were clearly present at midlevels of the ipsilateral LGNv, and labeled terminals were confined to the posterior portion of the nucleus.

Superior colliculus

In all cases, WGA-HRP labeled terminals were observed in the superior colliculus contralateral to the eye injection (Figs. 2, 5, 6). No labeled terminals were observed in the ipsilateral SC. In all cases patches of alternating high and low density of labeled terminals were located throughout the entire rostrocaudal extent of the SC. Terminals were predominantly confined to the superficial layers, I and II, and sparse labeling was observed in layer III.

Other retinorecipient nuclei

In all cases (Table 1), the contralateral pretectum contained densely packed terminals located mostly posterior and medial to LP and extending to the rostral level of the

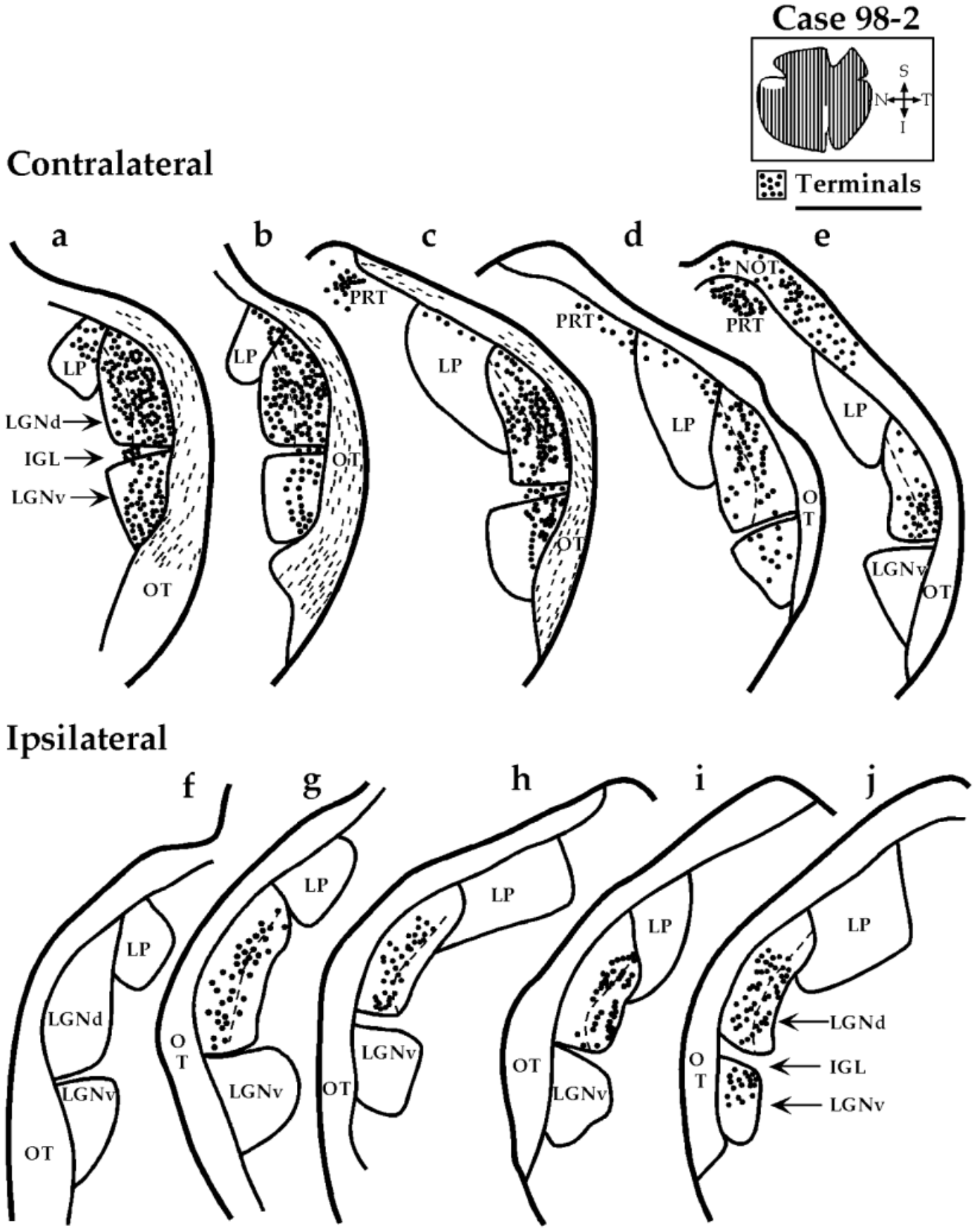

Fig. 3. Reconstructions of labeled retinal axon terminals in a coronally sectioned thalamus following an intraocular injection of WGA-HRP in case 98-2. In this case, the time allowed for transport of the tracer was 2 days. Labeling was most dense in the contralateral LGNd (**a–e**). In the rostral sections (a-c), labeling appears to fill the entire LGNd, whereas at more caudal levels, labeled terminals were sparse and did not occupy the entire nucleus. Ipsilateral projections to LGNd and LGNv (**f–j**) were distributed throughout the LGNd, with the zone immediately adjacent to the optic tract devoid of labeled terminals. Labeled retinal terminals were also observed in the contralateral LP and PRT. The inset, above right, is an illustration of the extent of uptake of the tracer in the retina (stippled). The injection covered virtually the entire retina. The thalamic sections are arranged from rostral (a,f) to caudal (e,j). Dots represent labeled axon terminals, and dashes represent portions of axons. Thick lines represent the border of the thalamus, and thin lines represent borders of individual thalamic nuclei. For abbreviations, see list. Dorsal is up.

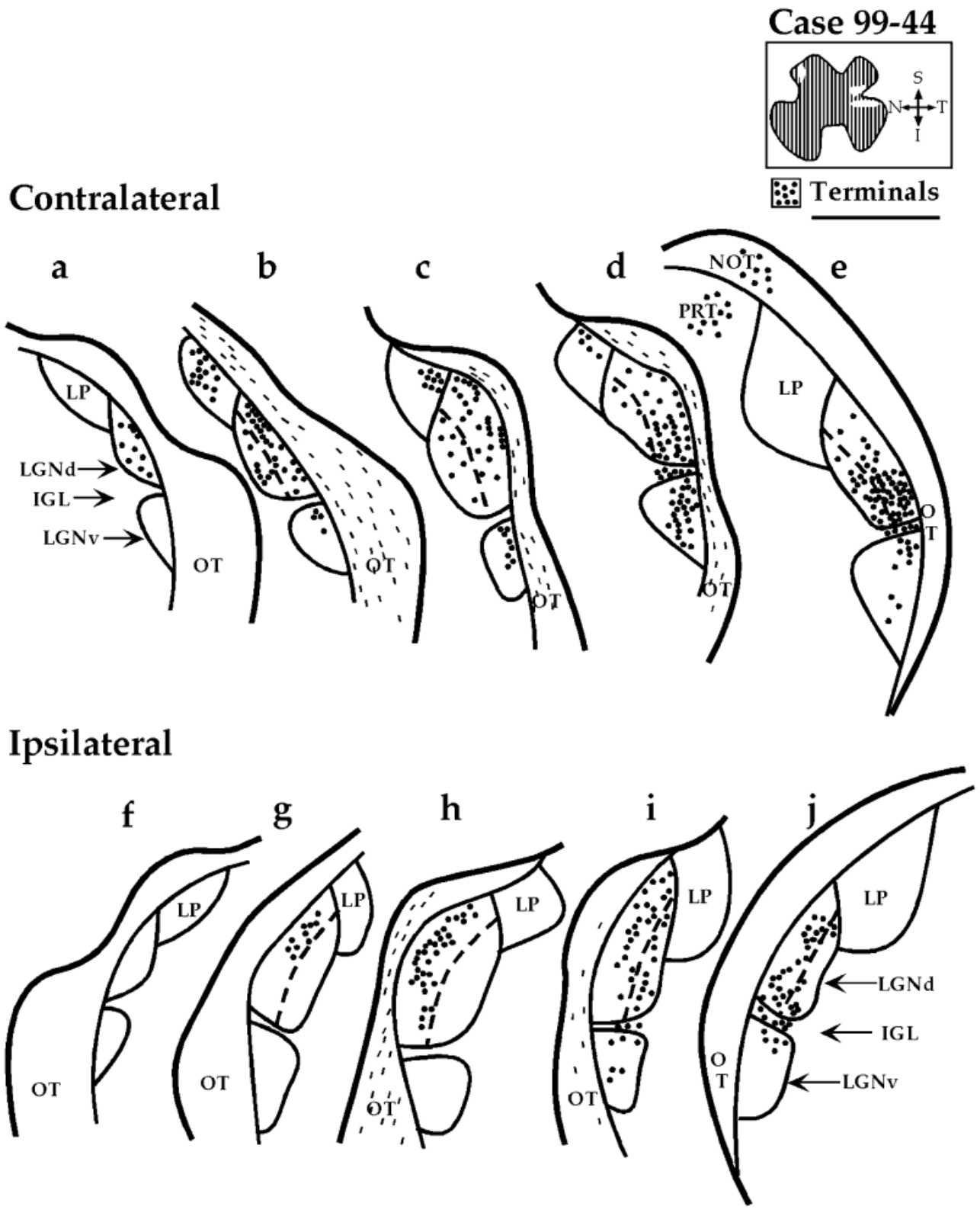

Fig. 4. **a–j:** Reconstructions of WGA-HRP-labeled axon terminals in a coronally sectioned thalamus following intraocular injection in case 99-44. In this case, 7 days were allowed for transport of tracer. Although the amount of labeled terminals was less dense than in case 98-2, labeling patterns were similar to other cases. Labeled axon terminals were observed in the contralateral LGNd, LGNv, LP, and PRT and in the ipsilateral LGNd and LGNv. For abbreviations, see list. Dorsal is up.

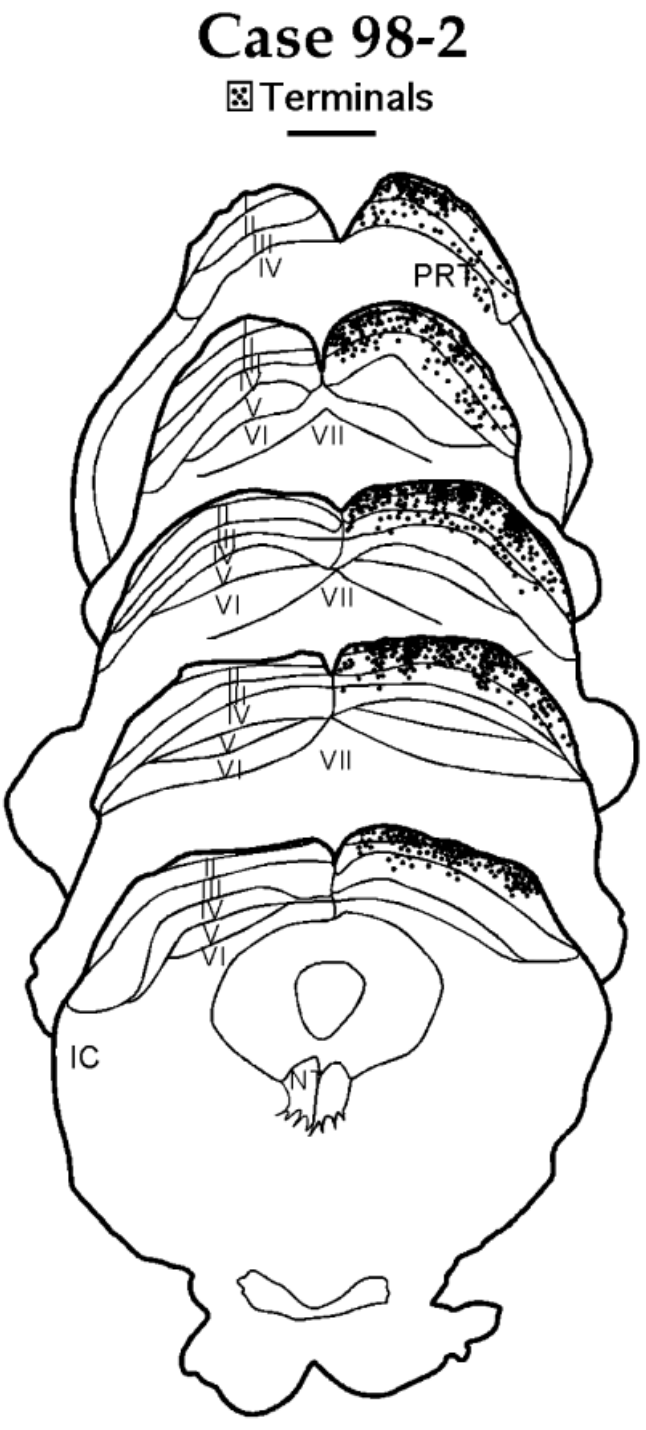

Fig. 5. Reconstruction of labeled retinal axon terminals in a coronally sectioned SC following intraocular injections of WGA-HRP in case 98-2. In this case, transport time allowed for the tracer was 2 days. Alternating patches of high and low density of labeled terminals were visible throughout the entire rostrocaudal extent in the superficial layers of the SC. Labeled terminals were also seen in the PRT. Labeled terminals were observed solely in the SC contralateral to the eye injection. Sections are arranged rostral (R, top section) to caudal (C, bottom). For abbreviations, see list. Dorsal is up.

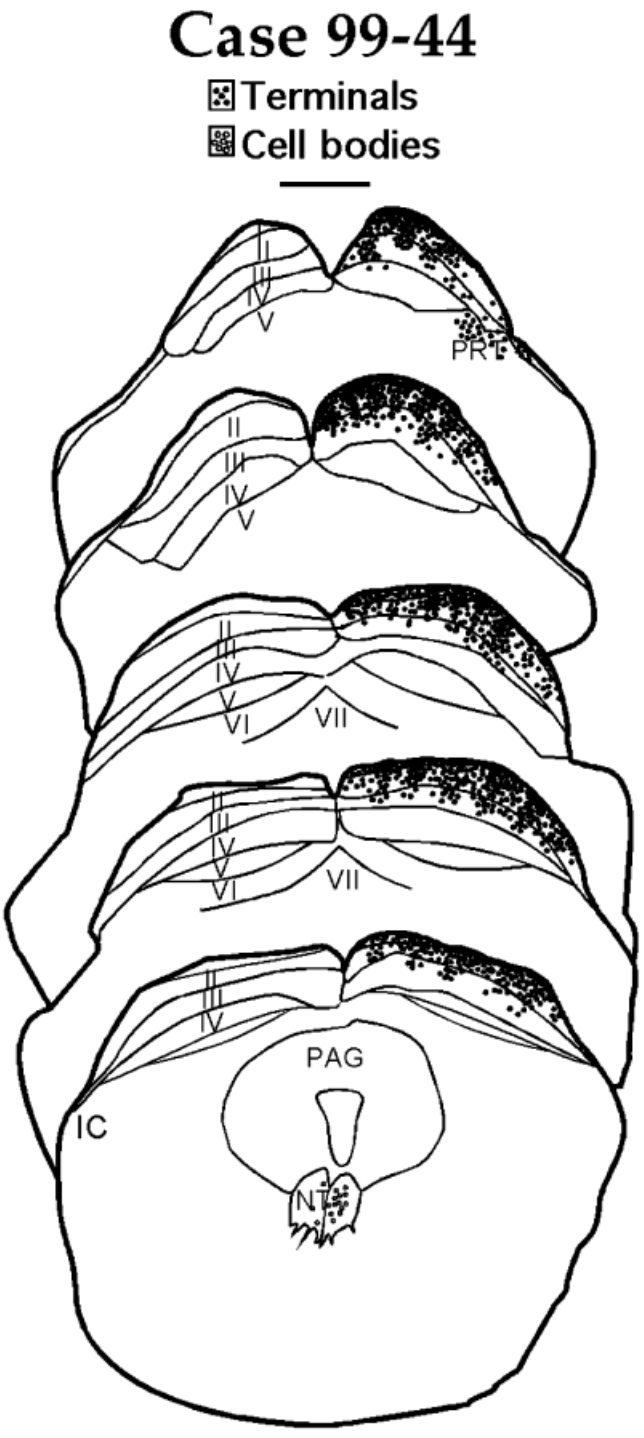

Fig. 6. Reconstruction of labeled retinal axon terminals in the coronally sectioned SC in case 99-44. Transport time of WGA-HRP was 7 days. Labeling patterns were very similar to those of the other cases, with alternating dense and light patches of labeled terminals in the superficial layers of the SC in the medial to lateral direction. As in case 98-14, labeled cells were observed in the NT. For abbreviations, see list. Dorsal is up.

SC (Figs. 3, 6). A population of labeled terminals of moderate density was also observed in the contralateral nucleus of the optic tract in three cases (Figs. 3e, 4e). In five of the six cases, labeled axon terminals were observed in the contralateral lateral posterior nucleus (LP; Figs. 3, 4). In four cases, the amount of staining was relatively sparse and located along its dorsal border. In one case (98-2), labeling was also observed in the contralateral medial terminal nucleus (MTN) of the accessory optic system (not shown). In this case, labeled retinal axon terminals were very dense and were located in the posterior region of the MTN, just bordering the cerebral peduncle. There were no labeled terminals observed in the ipsilateral MTN. Labeled cell bodies were observed bilaterally in the trochlear nucleus (NT) in two cases (Fig. 6). Unlike label observed in other subcortical nuclei, intensity of the label was not diminished in the 7-day group.

DISCUSSION

In the present investigation, intraocular injections in the marsupial *Monodelphis domestica* revealed that the dominant projections from the eye are to the contralateral dorsal lateral geniculate nucleus (LGNd) and superior colliculus (SC). Retinorecipient nuclei also include the contralateral LGNv, LP, and PRT. In a few cases, the ipsilateral LGNd and LGNv were also labeled. The lack of ipsilateral label in all cases is probably due to the differences in survival times and differences in the effective uptake of the tracer. In the following discussion, we compare patterns of retinal projections and thalamic architecture across marsupials and across mammals, and we suggest possible sources that contribute to the different types of neuroanatomical and structural organization of the LGNd in mammals.

Retinal projections in mammals

Superior colliculus. Dense projections from the retina to the contralateral SC have been observed in all marsupials investigated (Cavalcante et al., 1975; Pearson et al., 1976; Royce et al., 1976; Sanderson and Pearson, 1977; Sanderson et al., 1979), as well as all eutherians that have been studied (Campbell et al., 1967; Laemle and Noback, 1970; Tigges and Tigges, 1970, 1981; Wilson and Toyne, 1970; Graybiel, 1975; Cusick and Kaas, 1982; Florence et al., 1986; Dinopoulos et al., 1987; Uchimi et al., 1995). Although in most mammals, the densest projections are to the superficial layers of the SC, the pattern of projection varies. For instance, in most marsupials, terminal labeling in the contralateral SC is homogeneous (e.g., brush-tailed possum, Tasmanian devil, fat-tailed dunnart, Sanderson et al., 1978, 1979; Haight and Sanderson, 1988), unlike the patchy pattern observed in the present investigation. In other mammals, the patterns vary from relatively homogeneous (e.g., cat and galago) to patchy (e.g., macaque monkey; see Kaas and Huerta, 1988, for review).

The observation that labeled terminals were observed solely in the contralateral SC is different from that found in other mammals. In all marsupials studied, there is a small ipsilateral retinal projection to SC, although the laminar distribution varies across species (Cavalcante et al., 1975; Royce et al., 1976; Pearson et al., 1976; Sanderson and Pearson, 1977; Sanderson et al., 1979). Similarly, an ipsilateral retinal projection to the SC has been observed in all eutherian mammals studied (Campbell et al., 1967; Laemle and Noback, 1970; Tigges and Tigges, 1970, 1981; Wilson and Toyne, 1970; Graybiel, 1975; Cusick and Kaas, 1982; Florence et al., 1986; Uchimi et al., 1995), with the exception of the brown bat (Cotter, 1985). Even in more primitive mammals, such as the hedgehog (Dinopolous et al., 1987), and in mammals with very poorly developed visual systems, such as the blind mole rat (Cooper et al., 1993), retinal projections to the SC are bilateral. Thus, the lack of labeled terminals in the ipsilateral SC of the short-tailed opossum is surprising.

It is possible that the lack of labeling in the ipsilateral SC is the result of technical problems in transport of tracer. Another possibility is that our assessment of the total uptake of tracer in the retina was confounded by tissue damage or incomplete vitreous removal, both of which would have produced reaction product in the retina. Finally, the spacing of our TMB-reacted sections through the midbrain (160 μm apart) may have been too large to allow us to see sparse patterns of label. However, the presence of ipsilateral projections to the LGNd and LGNv (although sparse) in some cases argues against this.

Another possibility is that the lack of transport to the ipsilateral SC is a real feature of the *Monodelphis* brain and represents a primitive feature of organization that has been retained in *Monodelphis*. Support for this supposition comes from degeneration studies in monotremes and other nonmammalian vertebrates. In monotremes, an early mammalian radiation (see Fig. 7), virtually all the retinal ganglion cell axons project to the contralateral side. In particular, retinal projections to the SC in both the echidna and platypus are completely crossed (Campbell and Hayhow, 1971, 1972). In birds, reptiles, turtles, and amniotes, the retinotectal projection is completely crossed as well (Bass and Northcutt, 1981a, b; see Butler and Hodos, 1996, for review). Thus, one interpretation of our results is that a strict contralateral retinocollicular projection is a primitive feature that has been retained in extant monotremes and lost in all but a few species of marsupials, such as *Monodelphis*. An alternative interpretation is that the ipsilateral SC connections arose with the emergence of maruspials and was subsequently lost in some marsupials such as *Monodelphis*.

Lateral geniculate nucleus. Although results from the present investigation did not demonstrate clear regions of segregated contralateral and ipsilateral retinal projections within the LGNd, label was very patchy, and the contralateral projection was extremely dense. In other marsupials investigated, the degree to which inputs from the two eyes is segregated varies dramatically. For instance, there is a high degree of binocular overlap of inputs in the Virginia opossum (Benevento and Ebner, 1970), and the Tasmanian devil (Sanderson et al., 1979), much like the pattern observed in the present investigation. In other groups of marsupials including brown bandicoots (Haight and Sanderson, 1990), the grey kangaroo (Sanderson et al., 1984), and the Tasmanian potoroo (Sanderson et al., 1989; Wilson and Astheimer, 1989), retinal ganglion cell axons projected to eye-specific regions in the LGNd, although the degree of segregation of retinal inputs varied among different species of marsupials (Table 2).

Cytoarchitectural differences have also been observed in the LGNd of different marsupials. For instance in Virginia opossums (Royce et al., 1976; Wilson and Astheimer,

TABLE 2. Cytoarchitectural Lamination, Retinal Projection Patterns, Lifestyle, and Eye Placement in Marsupial LGNd[1]

Suborder Family *Genus, species*	Common name[2]	No. of cell layers[3] or segments	No. of RTR[4]	Binocular overlap[5]	Lifestyle
Polyprotodonta					
Didelphidae					
Didelphis virginanis	Virginia opossum	1	2	1	Omnivore
Didelphis aurita	American opossum	2	2	1	Omnivore
Monodelphis domestica	Short-tailed opossum	2	2	1	Omnivore
Marmosa mitts	S. American opossum	2	6	2	Omnivore
Didelphis marsupialis	Gambal	1	2	1	Omnivore
Dasyuridae					
Sarcophilus harrisii	Tasmanian devil	1	2	1	Predator/scavenger
Dasyurus hallucatus	Northern quoll	3	6	3	Predator
Dasyurus viverrinus	Eastern quoll	3	5	3	Predator
Sminthopsis crassicaudata	Fat-tailed dunnart	4	6	3	Predator
Dasyurides byrnei	Kowari	5	6	3	Predator
Peramelidae					
Isoodon obesulus	Brown bandicoot	1	3	0	Omnivore
Parameles gunnii	Barred bandicoot	1	2	0	
Diprotodonta					
Phalangeridae					
Trichosurus vulpecula	Brush-tail possum	4	7–8	1	Herbivore
Tarsipedidae					
Tarsipes rostratus	Honey possum	6	10	5	Herbivore
Macropodidae					
Bettongia gaimardi	Bettong	4	7	1	Omnivore
Potorous tridactylus	Potoroo	6	7	0	Herbivore
Marcopus eugenii	Tammar wallaby	6	9	0	Herbivore
Marcopus parma	Parma wallaby	N/A	9	0	Herbivore
Peradorcas concinna	Nabarlek	4	8	1	Herbivore
Thylogale billardierii	Pademelon wallaby	4	7–8	0	Herbivore
Wallabia bicolor	Swamp wallaby	4	9	0	Herbivore
Marcopus giganteus	Grey kangaroo	7	10	0	Herbivore
Phascolarditadae					
Phascolarctos cinereus	Koala	4	7–8	0	Herbivore
Acrobatidae					
Acrobates pygmaeus	Feather-tail glider	2	3	1	Omnivore
Petauridae					
Petarus breviceps	Sugar glider	4–5	7	0	Herbivore
Vombatidae					
Lasiorhinus latifrans	Hairy-nosed wombat	5	8	0	Herbivore
Vombatus ursinus	Common wombat	3	7	0	
Pseudocheiridae					
Pseudocheirus peregrinus	Ring-tail possum	1	5	0	Herbivore

[1]Modified from Haight and Sanderson, 1990.
[2]Parma wallaby, Nabarlek, Pademelon wallaby, forest wombat, koala, feather-tail glider, sugar glider, swamp wallaby, from Sanderson et al., 1987; brown bandicoot, barred bandicoot, from Haight and Sanderson, 1990; potoroo, pademelon wallaby, Tammar wallaby, grey kangaroo, Bettong, from Sanderson et al., 1984; kowari, fat-tailed dunnart, from Haight and Sanderson, 1988; brush-tailed possum, from Hayhow, 1967; Sanderson et al., 1978; Tasmanian devil, from Sanderson et al., 1979; gambal, from Lent et al., 1976; ring-tailed possum, from Pearson et al., 1976; Virginia opossum, South American opossum, from Royce et al., 1976; Eastern quoll, from Sanderson and Pearson, 1977; honey possum, from Harman et al., 1990; dunnart, from Dunlop et al., 1997.
[3]Number of cytoarchitectonic divisions of the LGNd.
[4]RTR, retinal terminal regions. Projection patterns of retinal ganglion cell axon terminals; number of discrete bands or regions of retinogeniculate input; this includes the number of eye-specific regions as well as regions that receive binocular input.
[5]Number of RTRs that receive input from both the ipsilateral and contralateral eyes.

1989), Tasmanian devils (Sanderson et al., 1979), and ring-tailed possums (Pearson et al., 1976) the LGNd is undifferentiated, with no clear α and β regions (Table 2). In other marsupials such as South American opossums, gambals, and bandicoots (see Table 2 and Haight and Sanderson, 1990, for review), the LGNd has only two cytoarchitectonically distinct segments (α and β). This is similar to the cytoarchitectonic appearance of the LGNd of the *Monodelphis*. Finally, in some marsupials the α segment contains discrete sublaminae. For instance, in kowaris, fat-tailed dunnarts (Haight and Sanderson, 1988), Tasmanian bettongs, Tasmanian potoroos, grey kangaroos (Sanderson et al., 1984), and brush-tailed possums (Hayhow, 1967; Sanderson et al., 1978) the α segment is divided into a number of cell layers, which gives the LGNd a distinct laminar appearance, whereas the β segment appears homogenous (Table 2). Thus, in marsupials, there are at least three types of cytoarchitectonic variations in the LGNd: a completely homogenous LGNd, an LGNd divided into α and β segments only, and an LGNd in which the α segment contains multiple laminae.

Not surprisingly, the presence of multiple cytoarchitectonic layers in the LGNd is often coincident with the presence of multiple retinal terminal regions (RTRs), whereas a relatively homogeneous LGNd is coincident with fewer RTRs (Table 2). For example, among the polyprodotont marsupials, the cytoarchitecture of the LGNd of the Virginia opossum (Royce et al., 1976) and the Tasmanian devil (Sanderson et al., 1979) is relatively simple, with no clear α and β subregions, and these animals have substantial overlap of retinal inputs. Other polyprodotont marsupials such as the kowari and fat-tailed dunnart (Haight and Sanderson, 1988), have slightly more complex LGNd cytoarchitecture, with four to five laminae and six retinal terminal regions. In most diprotodont marsupials, the LGNd is well laminated, with four to seven cytoarchitectonic laminae and three to ten RTRs with little or no binocular retinal terminal regions (Table 2; Sanderson et al., 1984; Sanderson et al., 1987; Haight and Sanderson, 1990).

In a variety of eutherian mammals, a similar correspondence exists between cytoarchitecture and segregation of retinal inputs in the LGNd. For instance, the LGNd of hedgehogs (Campbell et al., 1967; Dinopoulos et al., 1987), rabbits (Takahashi et al., 1977), microchiropteran bats (Pettigrew et al., 1989), and one species of tree shrew

(Simmons, 1979) consists of a fairly homogenous cell population with no obvious laminar arrangement. Examination of retinal projections to the LGNd in these animals indicates a large amount of overlap of projections from the ipsilateral and contralateral eye, with very few eye-specific retinal terminal bands or regions. In the rat LGNd, the α and β segments are relatively undifferentiated, but the retinal projections are segregated into separate, patchy regions (Cunningham and Lund, 1971; Lund et al., 1974; Reese, 1988). This concealed lamination described in rats is similar to the LGNd organization in the ring-tailed possum (Pearson et al., 1976) and the brown bandicoot (Haight and Sanderson, 1990), in which no clear cytoarchitectonic distinctions are apparent, yet projection patterns indicate at least some segregation of retinal inputs. Finally, in cats (Stone and Hansen, 1966; Peters and Paley, 1966) and primates (Kaas et al., 1978; Florence et al., 1986; see Kaas and Huerta, 1988, for review), the LGNd is differentiated into a number of cytoarchitectonic and eye-specific layers, although the number of laminae varies across these species. Thus, the three types of organization described above for marsupials are present in eutherian mammals as well.

Factors that contribute to lamination and eye-specific domains in the lateral geniculate nucleus of mammals

Comparative studies indicate that three general types of organization of the LGNd have evolved in the mammalian visual system, suggesting that there are a restricted number of factors that contribute to its organization. One source of current organization is genetic. If genes are responsible for the present organization of the LGNd, then one would predict that closely related species would have a similarly appearing LGNd organization. Marsupials are an order of mammals composed of two suborders, polyprotodonts and diprotodonts (Fig. 7; Table 2). Comparisons of closely related marsupials reveal that in polyprotodont marsupials the LGNd is organized in a less complex fashion than in diprotodonts. For example, polyprotodonts such as the Virginia opossum, Tasmanian devil, and brown bandicoot possess a cytoarchitectonically homogenous LGNd, and most other polyprotodonts have two or three laminae. Only the fat-tailed dunnart and kowari have more cytoarchitectonic laminae. Additionally, most polyprotodonts have a very high degree of binocular overlap of retinal projections (30–50% of RTR receive input from both eyes). There is evidence that the polyprotodonts represent an evolutionarily older lineage than diprotodonts (Richardson, 1988), suggesting that this reduced cytoarchitectonic and connectional segregation reflects a primitive feature of LGNd organization. This supposition is supported by studies in monotremes demonstrating that the LGNd is small and cytoarchitectonically homogenous (Campbell and Hayhow, 1971, 1972).

Diprotodonts, on the other hand, have an LGNd that is subdivided cytoarchitectonically into four to seven laminae, as well as a large number of RTRs, which receive input almost exclusively from one eye (Table 2). Thus, a comparative analysis reveals that in marsupials a predictor of LGNd organization is phylogeny. This observation is likely to be true for other mammals as well. For instance, although the organization and complexity of the LGNd varies across primates, as an order, the LGNd of primates is more complex than the LGNd in the order Rodentia. Thus, the complexity of the LGNd organization in terms of the number of laminae, RTRs, and segregation of inputs is, at least in part, genetically determined. However, within the two suborders of marsupials (and within other orders such as primates) variability still exists, suggesting that other factors contribute to the cytoarchitectonic and neuroanatomical organization of the structure in question.

Another factor believed to contribute to current organization is the ecological niche of different mammals, because mammals with similar environmental demands often adapt similar underlying neural organizations (Sanderson et al., 1984; Barton and Purvis, 1995). With respect to the visual system, one would predict that animals such as predators would have evolved morphological features such as eye placement and receptor type, and corresponding sensory systems that are more like each other than they are to mammals that have different lifestyles, such as herbivores.

A comparative analysis of lifestyle and LGNd organization in marsupials that have been examined does suggest that within a suborder, lifestyle is likely to contribute to some of the variability observed in LGNd organization in different species. For example, the predatory polyprotodont marsupials that have been studied range in size from approximately 15 g to 5 kg ; they are all terrestrial and nocturnal. In all of these species, the LGNd contains three to five cytoarchitectonic laminae, with the exception of the Tasmanian devil (Sanderson et al., 1979), compared with the lack of cytoarchitectonic distinctions (one to two laminae) of the LGNd of nonpredatory polyprotodonts (Table 2). Furthermore, examination of retinal terminal projection patterns in predatory and nonpredatory polyprotodont marsupials indicates that the LGNd of the predatory species has five or six RTRs, whereas nonpredatory polyprotodonts have two or three RTRs (Table 2; Sanderson and Pearson, 1977; Sanderson et al., 1979; Haight and Sanderson, 1988; Dunlop et al., 1997).

Although the LGNd organization of predatory polyprotodonts is more complex than that of nonpredatory polyprotodonts, the idea of a predatory lifestyle as a predictor of complex LGNd organization in mammals in general is weakened by observations of the diprotodont marsupials. The diprotodonts that have been studied are mostly herbivores, yet in almost all species, their LGNd is organized in a complex fashion, with four to seven cytoarchitectonic laminae and four to ten eye-specific retinal terminal regions. In only one of the diprotodont herbivores that have been studied (honey possum; Harman et al., 1990) does the input from both eyes converge in the same RTR.

Although lifestyle, because it determines peripheral morphology, does appear to contribute to current organization, the spontaneous and patterned activity that arises from particular receptor types, distributions, and use plays an important role in the establishment and refinement of connections, and in the initial wiring of primary afferents. There is a wealth of data on the role activity plays in establishing normal patterns of ocular dominance columns and orientation columns in primary visual cortex (Shatz and Stryker, 1978; Antonini and Stryker, 1993; Chapman et al., 1996; Katz and Shatz, 1996; see Sur et al., 1999, for review), as well as barrel fields in the primary somatosensory cortex of mice (Van der Loos and Woolsey, 1973; Welker and Van der Loos, 1986). At the level of the

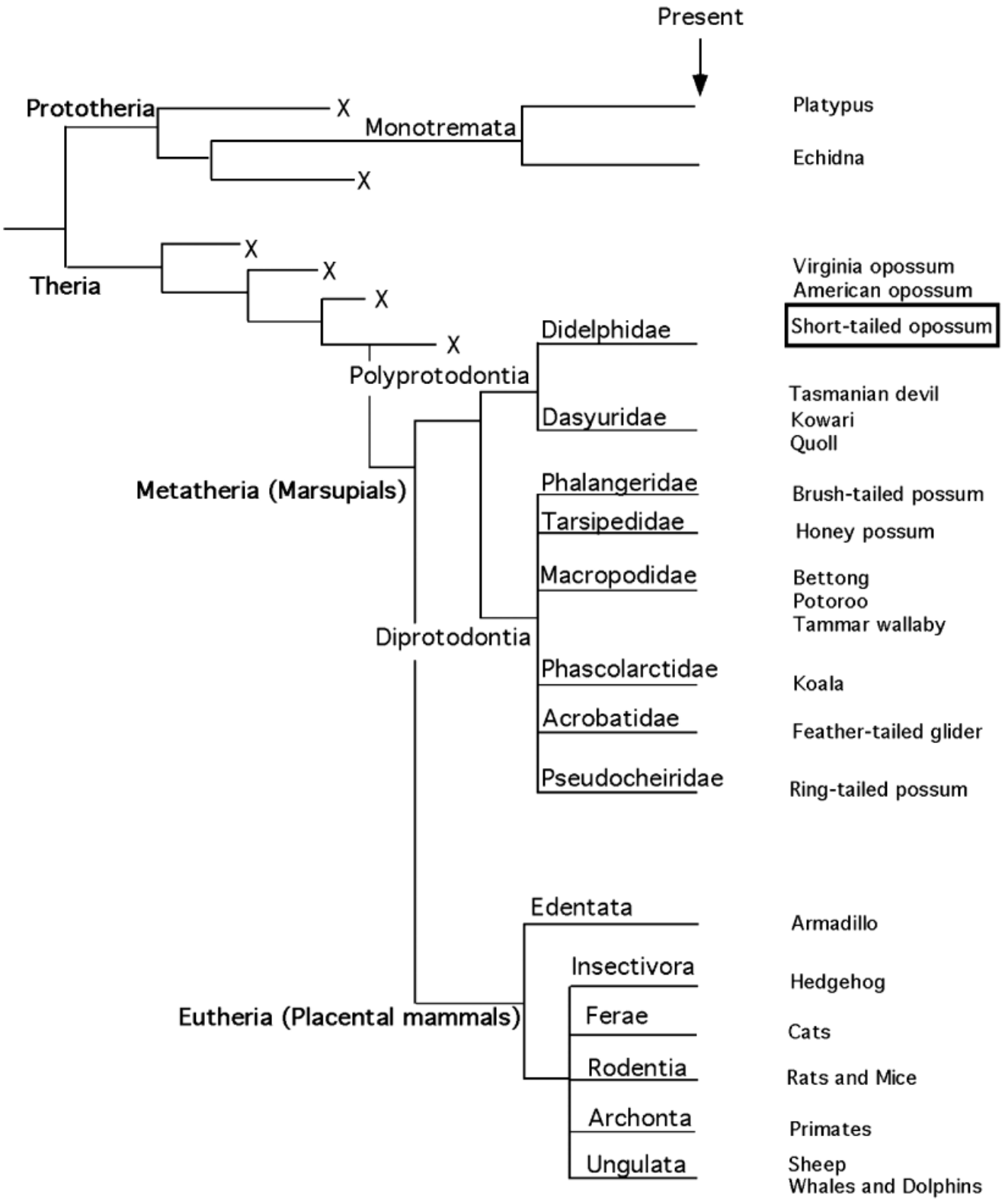

Fig. 7. A simplified cladogram depicting the relationship between the suborders of marsupials and other mammals (modified from Eisenberg, 1981). Prototherian mammals compose the oldest lineage, and only three species exist today. Metatherian mammals are thought to have emerged somewhat later (However, see Penny and Hasegawe, 1997, for an alternate interpretation) and Eutherian mammals later still. Xs denote lineages that are extinct.

dorsal thalamus, it is well established that activity-dependent competitive mechanisms are necessary for the formation of eye-specific laminae in the LGNd (see Shatz, 1990, for review). Both carnivores and primates have frontally placed eyes, and it is the competitive interaction of activity arising from visual stimulation from both eyes that modulates formation of laminae in the LGNd and of ocular dominance columns in V1 (Hubel and Wiesel, 1970; Hubel et al., 1977). However, although visual experience does modify ocular dominance columns, the initial formation of the columns occurs early in development, in the absence of visual stimulation (Wiesel and Hubel, 1974; Horton and Hocking, 1996).

From comparative studies, it is apparent that phenotypic variations observed in mammalian nervous system organization can be accounted for by some combination of phylogenetic relationship and lifestyle of the animal. Presumably changes in behavior and morphology associated with a particular lifestyle have a large impact on the activity patterns to which the developing nervous system is exposed. The genetic regulation of axonal development, when coupled with an activity pattern dictated by morphological features related to lifestyle (such as the location of the eyes on the head, receptor type and density, and nerve cell specialization within the retina), generates a particular type of LGNd organization observed in a species.

ACKNOWLEDGMENTS

We thank Elizabeth Disbrow, Barbara Chapman, and Deborah Hunt for helpful comments on this manuscript. We also thank Kelly Huffman for help with the experiments and Catherine Dunn for technical assistance. Leah Krubitzer was the recipient of NINDS grant 1 R01 NS35103-04A1.

LITERATURE CITED

Antonini A, Stryker MP. 1993. Rapid remodeling of axonal arbors in the visual cortex. Science 260:1819–1821.

Barton R, Purvis P. 1995. Evolutionary radiation of visual and olfactory brain systems in primates, bats and insectivores. Philos Trans R Soc Lond B Biol Sci 34:381–392.

Bass A, Northcutt R. 1981a. Retinal recipient nuclei in the painted turtle, *Chrsemys picta*: an autoradiographic and HRP study. J Comp Neurol 199:97–112.

Bass AH, Northcutt R. 1981b. Primary retinal targets in the Atlantic loggerhead sea turtle, *Caretta caretta*. Cell Tissue Res 218:253–264.

Benevento L, Ebner F. 1970. Pretectal, tectal, retinal and cortical projections to thalamic nuclei of the opossum in stereotaxic coordinates. Brain Res 18:171–175.

Brauer K, Schober W, Winkelmann E. 1978. Phylogenetical changes and functional specializations in the dorsal lateral geniculate nucleus (dLGN) of mammals. J Hirnforsch 19:177–187.

Brauer K, Schober W, Leibnitz L, Werner L, Luth H, Winkelmann E. 1984. The ventral lateral geniculate nucleus of the albino rat: morphological and histochemical observations. J Hirnforsch 25:205–36.

Butler A, Hodos W. 1996. Comparative vertebrate neuroanatomy. New York: John Wiley and Sons. p 235–256.

Campbell C, Hayhow W. 1971. Primary optic pathways in the echidna, *Tachyglossus aculeatus*: an experimental degeneration study. J Comp Neurol 143:119–136.

Campbell C, Hayhow W. 1972. Primary optic pathways in the duckbill platypus, *Ornithorynchus anatinus*: an experimental degeneration study. J Comp Neurol 145:195–208.

Campbell C, Jane J, Yashon D. 1967. The retinal projections of the tree shrew and hedgehog. Brain Res 5:406–418.

Carroll E, Wong-Riley M. 1984. Quantitative light and electron microscopic analysis of cytochrome oxidase-rich zones in the striate cortex of the squirrel monkey. J Comp Neurol 222:1–17.

Cavalcante L, Rocha-Miranda C, Lent R. 1975. Hypothalamic, tectal and accessory optic projections in the opossum. Brain Res 84:302–307.

Chapman B, Stryker MP, Bonhoeffer T. 1996. Development of orientation preference maps in ferret primary visual cortex. J Neurosci 16:6443–6453.

Chiel H, Beer R. 1977. The brain has a body: adaptive behavior emerges from interactions of nervous system, body and environment. Trends Neurosci 20:553–557.

Cooper H, Herbin M, Nevo E. 1993. Visual system of a naturally microphthalmic mammal: the blind mole rat, *Spalax ehrenbergi*. J Comp Neurol 328:313–350.

Cotter J. 1985. Retinofugal projections of the big brown bat, *Eptesicus fuscus* and the neotropical fruit bat, *Artibeus jamaicensis*. Am J Anat 172:105–124.

Cunningham T, Lund R. 1971. Laminar patterns in the dorsal division of the lateral geniculate nucleus of the rat. Brain Res 34:394–398.

Cusick C, Kaas J. 1982. Retinal projections in adult and newborn grey squirrels. Brain Res 4:275–284.

Dinopoulos A, Karamanlidis A, Michaloudi H, Antonopoulos J, Papadopoulos G. 1987. Retinal projections in the hedgehog (*Erinaceus europaeus*). An autoradiographic and horseradish peroxidase study. Anat Embryol 176:65–70.

Dunlop S, Tee L, Lund R, Beazley L. 1997. Development of primary visual projections occurs entirely postnatally in the fat-tailed dunnart, a marsupial mouse, *Sminthopsis crassicaudata*. J Comp Neurol 384:26–40.

Eisenberg JF. 1981. The mammalian radiations. An analysis of trends in evolution, adaptation, and behavior. Chicago: University of Chicago Press.

Florence S, Conley M, Casagrande V. 1986. Ocular dominance columns and retinal projections in New World spider monkeys (*Ateles ater*). J Comp Neurol 243:234–248.

Gallyas F. 1979. Silver staining of myelin by means of physical development. Neurol Res 1:203–209.

Gibson A, Hansma D, Houk J, Robinson F. 1984. A sensitive low artifact TMB procedure for the demonstration of WGA-HRP in the CNS. Brain Res 298:235–241.

Graybiel A. 1975. Anatomical organization of retinotectal afferents in the cat: an autoradiographic study. Brain Res 96:1–23.

Haight J, Neylon L. 1981. A description of the dorsal thalamus of the marsupial native cat, *Dasyurus viverrinus* (Dasyuridae). Brain Behav Evol 19:155–179.

Haight J, Sanderson K. 1988. Retinal projections in two Australian polyprotodont marsupials: kowari, *Dasyuroides byrnei*, and fat-tailed dunnart, *Sminthopsis crassicaudata* (Dasyuridae). Brain Behav Evol 31: 96-110.

Haight J, Sanderson K. 1990. An autoradiographic analysis of the organization of retinal projections to the dorsal lateral geniculate nucleus in two bandicoots *Perameles gunnii* and *Isoodon obesulus*; do bandicoots see like polyprotodonts or diprotodonts? Australian Mammal Society Symposium, Bandicoots and Bilbies. Melbourne, Victoria: Surrey Beatty and Sons.

Harman A, Coleman L, Beazley L. 1990. Retinofugal projections in a marsupial, *Tarsipes rostratus* (honey possum). Brain Behav Evol 36: 30–38.

Hayhow W. 1967. The lateral geniculate nucleus of the marsupial phalanger, *Trichosurus vulpecula*. An experimental study of cytoarchitecture in relation to the intranuclear optic nerve projection fields. J Comp Neurol 131:571–604.

Horton J, Hocking D. 1996. An adult-like pattern of ocular dominance columns in striate cortex of newborn monkeys prior to visual experience. J Neurosci 16:1791–1807.

Hubel D, Wiesel T. 1970. The period of susceptibility to the physiological effects of unilateral eye closure in kittens. J Physiology 206:419–436.

Hubel D, Wiesel T, LeVay S. 1977. Plasticity of ocular dominance columns in monkey striate cortex. Philos Trans R Soc Lond B Biol Sci 278:377–409.

Jones EG. 1985. The thalamus. New York: Plenum Press.

Kaas J, Huerta M. 1988. The subcortical visual system of primates. Comp Primate Biol 4:327–391.

Kaas J, Weber J, Harting J. 1978. Patterns of retinal terminations and

laminar organization of the lateral geniculate nucleus. J Comp Neurol 182:517–554.

Katz L, Shatz C. 1996. Synaptic activity and the construction of cortical circuits. Science 274:1133–1138.

Laemle L, Nobak C. 1970. The visual pathways of the lorisid lemurs (*Nycticegbus coucang* and *Galago crassicaudatus*). J Comp Neurol 138: 49–62.

Lent R, Cavalcante L, Rocha-Miranda C. 1976. Retinofugal projections in the opossum; an anterograde degeneration and radioautographic study. Brain Res 107:9–26.

Lund RD, Lund JS, Wise RP. 1974. The organization of the retinal projection to the dorsal lateral geniculate nucleus in pigmented and albino rats. J Comp Neurol 158:383–403.

Mesulam M, Hegarty E, Barbas H, Carson K, Gower E, Knapp A, Moss M, Mufson E. 1980. Additional factors influencing sensitivity in the tetramethyl benzidine method for horseradish peroxidase neurohistochemistry. J Histochem Cytochem 28:1255–1259.

Nieuwenhuys R. 1994. The neocortex. An overview of its evolutionary development, structural organization and synaptology. Anat Embryol 190:307–337.

Pearson L, Sanderson K, Wells R. 1976. Retinal projections in the ringtailed possum *Pseudocheirus peregrinus*. J Comp Neurol 170:227–240.

Penny D, Hasegawe M. 1997. The platypus put in its place. Nature 387: 549–550.

Peters A, Palay S. 1966. The morphology of laminae A and A1 of the dorsal nucleus of the lateral geniculate body of the cat. J Anat 100:451–486.

Pettigrew JD, Robson SK, Hall LS, McAnally KI, Cooper HM. 1989. Phylogenetic relations between microbats, megabats and primates (Mammalia: Chiroptera and Primates). Philos Trans R Soc Lond B Biol Sci 325:489–559.

Reese B. 1988. 'Hidden lamination' in the dorsal lateral geniculate nucleus: the functional organization of this thalamic region in the rat. Brain Res 472:119–137.

Richardson B. 1988. A new view of the relationships of Australian and American marsupials. Aust Mammalogy 11:71–74.

Royce G, Ward J, Harting J. 1976. Retinofugal pathways in two marsupials. J Comp Neurol 170:391–413.

Sanderson K, Pearson L. 1977. Retinal projections in the native cat, *Dasyurus viverrinus*. J Comp Neurol 174:347–357.

Sanderson K, Pearson L, Dixon P. 1978. Altered retinal projections in brushtailed possum, *Trichosurus vulpecula*, following removal of one eye. J Comp Neurol 180:841–868.

Sanderson K, Pearson L, Haight J. 1979. Retinal projections in the Tasmanian devil, *Sarcophilus harrisii*. J Comp Neurol 188:335–345.

Sanderson K, Haight J, Pettigrew J. 1984. The dorsal lateral geniculate nucleus of macropodid marsupials: cytoarchitecture and retinal projections. J Comp Neurol 224:85–106.

Sanderson K, Nelson J, Crewther D, Crewther S, Hammond V. 1987. Retinogeniculate patterns in diprotodont marsupials. Brain Behav Evol 30:22–42.

Shatz C. 1990. Competitive interactions between retinal ganglion cells during prenatal development. J Neurobiol 21:197–211.

Shatz CJ, Stryker MP. 1978. Ocular dominance of layer IV of the cat's visual cortex and the effects of monocular deprivation. J Neurophysiol (Lond) 218:267–283.

Simmons R. 1979. The diencephalon of *Ptilocercus lowii* (pen-tailed treeshrew). J Hirnforsch 20:69–92.

Stone J, Hansen S. 1966. The projection of the cat's retina on the lateral geniculate nucleus. J Comp Neurol 126:601–624.

Sur M, Angelucci A, Sharma J. 1999. Rewiring cortex: the role of patterned activity in development and plasticity of neocortical circuits. J Neurobiol 41:33–43.

Takahashi E, Hickey T, Oyster C. 1977. Retinogeniculate projections in the rabbit: an autoradiographic study. J Comp Neurol 175:1–12.

Tigges M, Tigges J. 1970. The retinofugal fibers and their terminal nuclei in *Galago crassicaudatus* (primates). J Comp Neurol 138:87–102.

Tigges J, Tigges M. 1981. Distribution of retinofugal and corticofugal axon terminals in the superior colliculus of squirrel monkey. Invest Ophthalmol Vis Sci 20:149–158.

Uchimi O, Sugita S, Fukuta K. 1995. Retinal projections to the subcortical nuclei in the Japanese field vole (*Microtus montebelli*). Exp Animal 44:193–203.

Van der Loos H, Woolsey TA. 1973. Somatosensory cortex: structural alterations following early injury to sense organs. Science 179:395–398.

Welker E, Van der Loos H. 1986. Is areal extent in sensory cerebral cortex determined by peripheral innervation density? Exp Brain Res 63:650–654.

Wiesel TN, Hubel DH. 1974. Ordered arrangement of orientation columns in monkeys lacking visual experience. J Comp Neurol 158:307–318.

Wilson M, Toyne M. 1970. Retino-tectal and cortico-tectal projections in *Macaca mulatta*. Brain Res 24:395–406.

Wilson P, Astheimer L. 1989. Laminar and non-laminar patterns of acetylcholinesterase activity in the marsupial lateral geniculate nucleus. Brain Res 486:236–260.